

Urban Building Energy Modeling to Support Climate-Sensitive Planning in the Suburban Areas of Santiago de Chile

Original

Urban Building Energy Modeling to Support Climate-Sensitive Planning in the Suburban Areas of Santiago de Chile / Mutani, Guglielmina; Alehasin, Maryam; Yang, Huisi; Xiaotong, Zhang; Felmer, Gabriel. - In: BUILDINGS. - ISSN 2075-5309. - ELETTRONICO. - 14:1(2024), pp. 1-23. [10.3390/buildings14010185]

Availability:

This version is available at: 11583/2984977 since: 2024-01-11T18:32:25Z

Publisher:

MDPI

Published

DOI:10.3390/buildings14010185

Terms of use:



This article is made available under terms and conditions as specified in the corresponding bibliographic description in the repository

Publisher copyright

(Article begins on next page)

Article

Urban Building Energy Modeling to Support Climate-Sensitive Planning in the Suburban Areas of Santiago de Chile

Guglielmina Mutani ^{1,*}, Maryam Alehasin ¹, Yang Huisi ², Zhang Xiaotong ² and Gabriel Felmer ²

¹ Department of Energy, Politecnico di Torino, Corso Duca degli Abruzzi 24, 10129 Torino, Italy; maryamalehasin@gmail.com

² Instituto de la Vivienda Facultad de Arquitectura y Urbanismo, Universidad de Chile, Portugal 84, Santiago 8330111, Chile; yanghuisi2333@gmail.com (Y.H.); ginziazhang@gmail.com (Z.X.); gfelmer@uchile.cl (G.F.)

* Correspondence: guglielmina.mutani@polito.it; Tel.: +39-0110904529

Abstract: Greenhouse gas emissions depend on natural and anthropic phenomena; however, to reduce emissions, we can only intervene in terms of anthropic causes. Human activity is very different in various countries and cities. This is mainly due to differences in the type of urban environment, climatic conditions, socioeconomic context, government stability, and other aspects. Urban building energy modeling (UBEM), with a GIS-based approach, allows the evaluation of all the specific characteristics of buildings, population, and urban context that can describe energy use and its spatial distribution within a city. In this paper, a UBEM is developed using the characteristics and consumption of eight typical buildings (archetypes) in the climate zone of Santiago de Chile. The archetype-based UBEM is then applied to the commune of Renca, a critical suburb of Santiago, with the use of QGIS to analyze the energy demand for space heating and the potential for energy saving after four retrofitting interventions. Knowing the costs of the retrofitting interventions and the energy price, the simple payback time was evaluated with the reduction in GHG emissions. Starting from the actual building stock, the results show that the most effective retrofitting intervention for the commune of Renca is the thermal insulation of walls and roofs; due to the type of dwellings, this particular intervention could be more convenient if associated with the installation of solar technologies. This methodology can be replicated with the data used by urban planners and public administrations available for many Chilean cities and in other countries.

Keywords: urban building energy modeling; building archetypes; energy performance; energy savings; retrofitting interventions; GHG emissions; energy policy; economic incentives; GIS; Chile



Citation: Mutani, G.; Alehasin, M.; Huisi, Y.; Xiaotong, Z.; Felmer, G. Urban Building Energy Modeling to Support Climate-Sensitive Planning in the Suburban Areas of Santiago de Chile. *Buildings* **2024**, *14*, 185. <https://doi.org/10.3390/buildings14010185>

Academic Editors: Debora Anelli, Pierluigi Morano, Marco Locurcio and Francesco Tajani

Received: 26 October 2023
Revised: 3 January 2024
Accepted: 6 January 2024
Published: 11 January 2024



Copyright: © 2024 by the authors. Licensee MDPI, Basel, Switzerland. This article is an open access article distributed under the terms and conditions of the Creative Commons Attribution (CC BY) license (<https://creativecommons.org/licenses/by/4.0/>).

1. Introduction

Over the last quarter of a century, global energy consumption has risen by 45%, and it is expected to further increase in the next quarter due to rapid growth in all regions of the developing countries in the Global South [1]. As a result of the escalating climate crisis, energy poverty has become one of the most serious threats to sustainable urban development. A decade ago, energy poverty was only seen as an issue in rich countries [2–4]; today, it is increasingly recognized as a widespread global phenomenon, and increasing attention is being given to energy transition and equity in developing countries [5–7]. Energy poverty is broadly defined as a household's inability to attain modern domestic energy services [7–9]; the links between energy poverty and urban planning are just beginning to be explored as emerging narratives in Asia [10], Africa [11], and Latin America [12,13] unveil a plethora of deep-rooted causes and disciplinary gaps to be bridged [14]. Among the latter, informal urban development, limited population data, and a lack of sufficient resources in developing countries pose several challenges in terms of finding ways to tackle energy poverty at an urban or territorial scale [15,16].

The case study of the suburbs of big cities in Chile is particularly interesting when it comes to energy poverty as thermally inefficient housing, low incomes, and a high dependency on fossil fuels, with resulting acute environmental and public health issues [17–20].

Over the last three decades, Chilean statistics have shown that residential energy consumption is responsible for over a third of primary energy consumption [21], leading government authorities to enforce residential building thermal regulations in 2000 for insulated roofs, and in 2007 for walls and floors [22]. Then, in 2023, high levels of airborne particulate matter in several cities of central and south-central Chile [23–25] led the government to enact an atmospheric decontamination plan (ADP) with more stringent energy savings and clean energy regulations [26]. This was aimed especially at reducing residential space heating, which accounts for over half of the country's residential energy use [21,27].

With the ever-increasing global energy consumption and soaring energy prices, urban building energy modeling (UBEM) has gained standing in the field of urban energy planning, and geographic information systems (GISs) have aided urban planners and policymakers in understanding the spatial dimension of energy uses [28]. However, further research efforts are needed to make the most of GIS tools and datasets for energy planning, especially in informal urban settlements in developing countries where limited building performance and energy consumption data are available.

In this study, archetype-based urban building energy modeling (UBEM) was developed with a GIS-based approach to evaluate the energy consumption of residential buildings within the commune of Renca, a poor suburb of Santiago de Chile. The energy consumption of typical buildings (archetypes) was implemented in the UBEM. This is a mainstream bottom-up approach when a consumption database for buildings is not available for city-scale applications [29]. Currently, accessibility of consumption data is one of the main limitations on energy modeling at an urban scale, and UBEM based on archetypes is widely used due a very limited amount of consumption data to provide, its simple approach and reduced modeling efforts [30]. On the other hand, the heterogeneities in terms of energy use and the possibilities of retrofitting interventions in buildings within complex urban environments cannot be detected [31,32].

1.1. Literature Review

Archetypes are mainly implemented in urban building energy modeling (UBEM), utilizing their annual energy-use intensity (EUI) with the aim of evaluating energy consumption, energy savings after retrofitting measures, and climate change's effects [30]. However, they are also used for life cycle assessment modeling to measure environmental impact and for indoor environmental quality modeling to evaluate indoor conditions and their impact on the occupants.

Building archetypes are characterized by the EUI, which describes the annual energy performance or the energy use normalized by the dimension of a building, per unit of floor area or per volume. This considers only the mainly characteristics of a building, envelope, and technological systems, excluding the influence of its size. Usually, archetypes are selected by the type of use, geometry, materials, systems, and occupants' behavior [33,34]. The use of census and cadastral data has been adopted by many scientists to study urban energy-use, integrate other energy-related variables, and then improve energy modeling and strategies to reduce consumptions and greenhouse gas emissions [35,36]. The EUI of archetypes can be modeled in UBEM with process-driven tools (e.g., Design-Builder [37], EnergyPlus [29,34,38], IDA ICE [37]), or with data-driven analyses using measured data [38–40] or energy performance certificate (EPC) databases [37,41]. Similarly, the EUI of archetypes can also be evaluated after energy-saving interventions and applied on an urban scale.

For urban/territorial analyses, the use of Geographic Information System (GIS) allows for the collection, evaluation, and management of geo-localized information about the characteristics of buildings, population, urban/territorial context, and local climatic conditions. Utilizing GIS, UBEM can effectively integrate archetype data, enabling the comprehensive

modeling and description of the EUI of buildings. This approach facilitates the spatial representation of all pertinent information about buildings on an urban scale [42].

In the literature, there are many studies that have used the building archetype technique to describe the energy use of building stock in a city, region, or country. Most of them have had the objective of describing the built environment (mainly in terms of residential buildings), evaluating the most effective efficiency measures and savings in energy, costs, and greenhouse gas (GHG) emissions. One of the best-known projects on archetypes in Europe was Tabula, which described the significant room for improvement in terms of energy use in buildings in European countries [43]. In Canada, some studies regarding archetypes allowing bottom-up modeling with the evaluation of energy demand, and the potential energy savings are available online [4,44]. In 2024, Osman et al. used Canadian household archetypes to evaluate energy savings with a demand–response control measure and obtained a load reduction of up to 69% in urban areas [45]. In two cities in the metropolitan area of Chicago, archetype-based UBEM was used as a policy support tool for energy planning on an urban scale [38]. The use of demographic and socioeconomic features allowed building archetypes to be refined for better application on an urban scale. Archetypes were also used for rural residential buildings in Kyrgyzstan (Central Asia) to analyze their status, evaluate potential energy savings, and study retrofitting strategies [34]. In Changsha City, GIS datasets were used to identify 22 archetypes from three periods of construction for a process-driven UBEM to calculate energy use and emission reduction [29]; these archetypes can be applied to many other Chinese cities. In Jordan, the energy performance of residential buildings was evaluated using three main archetypes; retrofitting interventions and the use of photovoltaic panels resulted in energy savings of 70% [46]. In a district of Kuwait City, the importance of the period of construction and occupants' behavior in the identification of archetypes was demonstrated [47].

In Europe, archetype-based UBEM has been widely used. A recent study includes data-driven and process-driven UBEMs based on archetypes for the city of Stockholm using a very rich dataset of information [37]; Stockholm aims to become fossil-fuel free by 2040, and the energy savings potential after seven retrofitting interventions and an electric heating scenario were analyzed. In Dublin, four residential archetypes were identified using the EPC database and implemented in two data-driven UBEMs to be applied on an urban scale [40]; the use of the segregation method reached an accuracy of 91%, and this modeling was used to evaluate retrofitting and climate-change scenarios. In Scotland, 24 archetypes were used to review the “energy efficiency standard for social housing” and to reach zero emissions from heating by 2045 [32]. In Italy, previous studies with archetype- and GIS-based UBEM approaches were applied for the cities of Turin [48] and Milan [42]. GIS-based UBEM allows for scaling up characteristics, energy-uses and energy savings of buildings to the urban scale, considering also urban features such as the socio-economic conditions of population and the building density of the built environment.

1.2. Research Objectives

In general, Chile has a strong economy and high income, but 30% of the population is economically vulnerable and income inequality is high. In countries like Chile, there is a growing awareness among central and local government authorities about the planning of urban housing because this has a strong impact on household energy intensity, and thus on the related social, financial, and environmental burdens [49]. As already mentioned, since 2000, many regulations have been approved to reduce energy consumption and its impact on the environment, up to the very recent atmospheric decontamination plan in 2023 [22,26].

The aim of this study is to model the energy consumption of buildings in the critical suburbs of the city of Santiago and to define a decision-support assessment combining the benefits of an archetype-based UBEM with a GIS-based UBEM. For Chilean buildings, eight archetypes are identified with their main energy-related variables and EUIs before and after retrofitting interventions. The GIS is used for collecting and integrating data to create a

complete geodatabase for energy modeling and to represent the results. The representation with graphs and maps of energy-related variables and EUI allows for better understanding of the spatial distribution of energy use. Archetype- and GIS-based UBEM is a user-friendly and replicable opportunity to involve all stakeholders in fostering sustainable development in cities; public administrations can evaluate the real specific potential of energy saving, and private citizens and companies can determine the effect of their actions for themselves and for the community.

This study was applied to Renca to analyze the energy performance of building stock as well as to propose and assess retrofitting interventions to reduce space-heating energy use in the poor outskirts of Santiago de Chile. The retrofitting measures proposed include the replacement of windows (frames and glasses) and thermal insulation on walls, roofs, and slabs. The Chilean administration wants to first reduce consumption with passive interventions and then produce energy through renewable sources; the installation of solar collectors could be a solution to be considered with the retrofitting of the roofs, at least to produce domestic hot water. Then, at a later stage, the current boilers could be replaced with heat pumps supplied by photovoltaic modules or with a district heating system connected to a cogeneration system.

This study can be used to drive energy retrofitting actions and policy recommendations, considering the typology of built environment, costs of retrofitting interventions, fuel price, and energy savings and reduction in GHG emissions.

2. Renca and the District of José Miguel Carrera CD-3

The residential building sector in Chile is responsible for over a third of the primary energy use and greenhouse gas (GHG) emissions [27,50]. This is partly explained by the fact that most buildings are residential, with 70% being old buildings [51]. However, the thermal inefficiency of housing has led to a large dependence on fossil fuels, particularly for domestic space heating, which accounts for over 50% of residential energy use [52]. The thermal inefficiency of Chilean housing stock is responsible for acute energy poverty [6], high levels of urban air pollution [17], high concentration of indoor combustion gases [23], high exposure to cold air temperatures [53], and an excess of seasonal infections and mortality due to respiratory and cardiovascular diseases [54].

Santiago, the capital and the largest urban center of Chile, has a critical level of air pollution because it is in a valley surrounded by mountains that limit ventilation. In the suburban areas of Santiago, low income and high fuel prices, combined with urban sprawl and low-quality housing, exacerbate household vulnerability together with fuel poverty and climate-related events. For the national residential climate zoning standard [55], Santiago (latitude 33° S) is in the central interior (CI) region of the country, which is characterized by a temperate Mediterranean climate with cold winters and mild summers. However, due to the high dependence on imported fossil fuels and the poorly insulated housing stock, the recent rise in fuel prices has worsened energy poverty with a serious concern for the public administration [56].

Renca is a low-income commune located on the northwestern outskirts of Santiago (Figure 1), which predominantly consists of low-density residential building stock. In Renca, the built-up areas are mostly residential, accounting for more than 40,000 dwellings located between the northern flank of the Mapocho River and the southern foothills of the Renca Hill (at 900 m a.s.l.). In the city, the buildings are mainly built before 2001 (about 84%); this study focuses also on the old residential district of José Miguel Carrera, called “district three” (CD-3) [57]. Figure 1 shows district CD-3 with an extension of nearly 80 hectares and it has two distinct areas: a zone with low-rise single-family houses built before 1940 (CZ-1/CZ-3) and a low- to mid-rise residential zone (CZ-2) mostly composed of condominiums built after the 1970s.

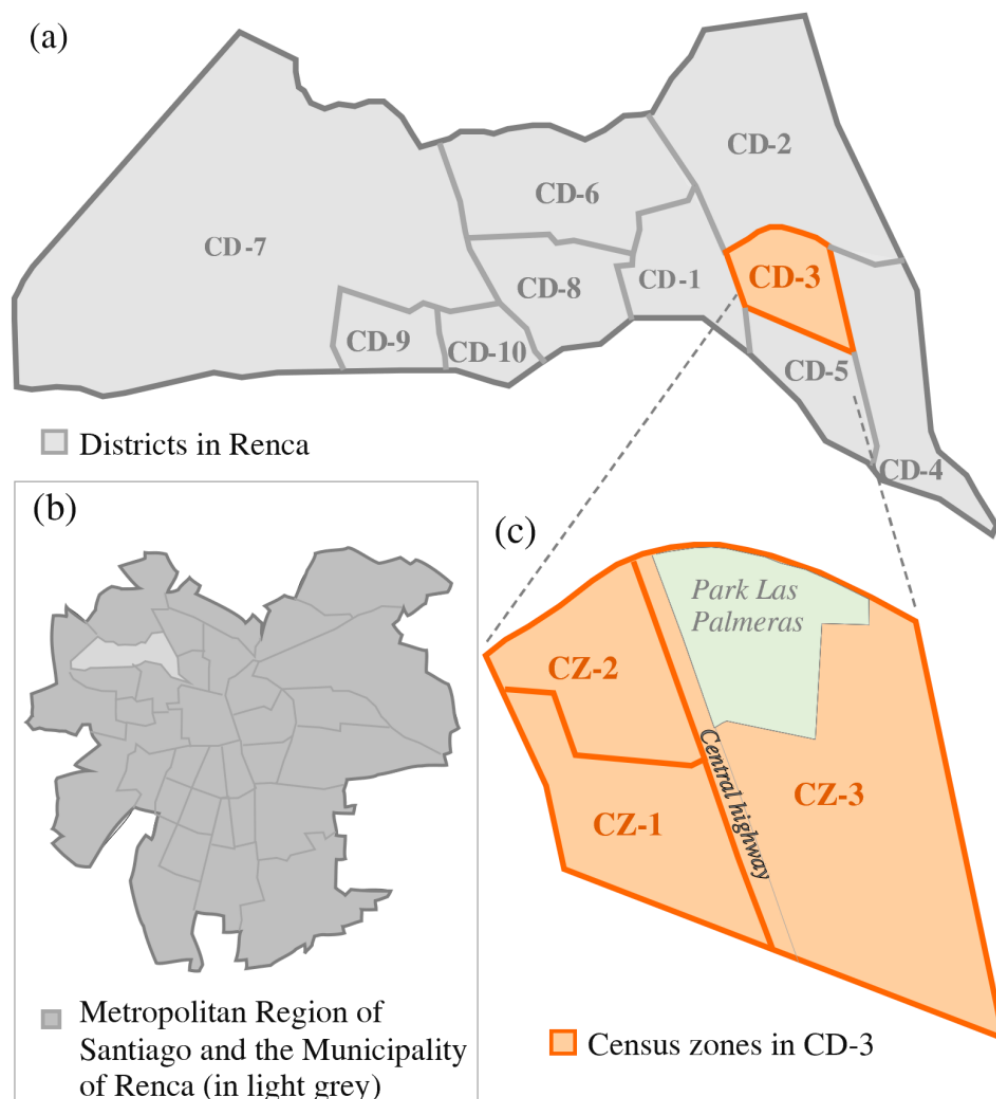


Figure 1. The geopolitical divisions: (a) Commune of Renca; (b) Metropolitan Region of Santiago “Gran Santiago”; (c) Census section zones of CD-3 “José Miguel Carrera” District.

2.1. Weather Data Characterization

Renca is located within a mountainous valley and has a mild climate with high diurnal temperature fluctuations that lead to high space-heating loads, especially in residential buildings. Based on hourly data from the Pudahuel weather station (national code n. 330021) [58], monthly diurnal outdoor air temperatures are over 10 °C higher than the nighttime temperatures. During the typical cold and warm season days, the peak of outdoor temperatures ranges between 0 and 15 °C, and 15 and 30 °C, respectively.

Chile is divided into seven climate zones (Zonas Termica ZT) according to the heating degree days (HDDs), and Renca is in climate zone ZT 3 with 1400 HDDs at 18 °C and 80 cooling degree days (CDDs) at 26 °C [58]. Thus, over a period of three to four months during winter, underheating becomes a danger to low-income inhabitants who have to choose between compromising their thermal comfort, health, and indoor air-quality over their expenses.

The weather data used in this study are reported in Table 1 and were mainly drawn from the Chilean Meteorological Office (Dirección Meteorológica de Chile DMC) [58]. The choice of 2017 as the reference year was guided by having consistency with data on buildings, population, and energy consumption data. In fact, these data were quite

stable because they were not influenced by the COVID-19 pandemic (2019–2020) and the subsequent energy crisis (2021–2022) due to the war between Russia and Ukraine.

Table 1. Renca climate data for the year 2017 (data refer to the weather station of Pudahuel; the data with * refer to PVGIS website*).

Month	Average Air Temperature (°C)	Solar Irradiation (kWh/m ²) *	Diffuse-to-Global Irradiation (%) *	Cloud Cover (%)	Air Relative Humidity (%)	Wind Speed (m/s)	Daily Hours of Light (h)
1	21.5	281.86	12	40	49.7	3.6	14.5
2	20.5	212.11	17	39	55.1	3.2	13.8
3	18.8	201.74	16	44	57	2.7	12.8
4	14.6	136.99	22	59	65.8	2.2	11.6
5	10.8	86.85	33	75	73.4	1.7	10.4
6	8.6	71.63	30	73	77.7	1.6	9.9
7	8.4	92.21	24	70	77.4	1.7	9.8
8	9.8	111.56	25	64	75.4	1.9	10.4
9	11.6	146.76	28	64	71.3	2.2	11.4
10	15	204.83	24	49	63	2.7	12.5
11	17.4	234.01	20	32	55.9	3.2	13.6
12	20	277.03	16	41	51.3	3.6	14.4

2.2. The Residential Building Stock in Renca

Renca has mainly low- to mid-rise residential buildings built on brick masonry (69% [59]) before the enforcement of the Chilean thermal regulations [60]. Over 68.5% of the housing stock is comprised of single-family houses, 24.4% are two-story houses, 7% are flats in three-, four-, or five-story apartment blocks, and 0.1% are condominiums with more than 5 floors (only 21 buildings). Almost all of the housing stock (83.8%) was built before the enforcement of the thermal regulation, that is, before 2001 (period R0); after 2001, a minimum of thermal insulation was established for roofs, from 2001 to 2007 (period R1); then, from 2007, thermal insulation was extended to include external walls and floor slabs (period R2) [59]. The district of CD-3 in José Miguel Carrera is similar but 95% of residential buildings were built before 2000 (period R0).

Based on recent statistics for the central interior region of Chile, the dominant energy sources for space heating in residential buildings are fossil fuels with liquefied petroleum gas (40%), paraffin (35%), electricity (12%), natural gas (7%), and firewood (4%) [53]. Such an extensive use of fossil fuels makes the reduction of energy consumption even more urgent.

3. Material and Methods

In this study, the GIS-based approach has been adopted to implement energy modeling on an urban scale, considering the buildings as territorial units. To geo-localize and collect all the information and to calculate–evaluate the specific features of each building, the geographic information system QGIS 3.16.11 was adopted. The decision to employ QGIS 3.16.11 stems from its status as open-source software, coupled with its recent stability and advanced features. This version proves instrumental in seamlessly utilizing and managing urban plan data stored in shapefiles, thereby enhancing the spatial geodatabase for the UBEM.

The methodological workflow was implemented to model and apply the EUI of the existing building stock in Renca and district CD-3, as shown in Figure 2, in three steps.

Step 1. Data collection. The characteristics of buildings that can influence energy consumption were determined using:

- the cadaster of housing and population (2017) from the National Service of Internal Affairs (Servicio de Impuestos Internos, SII);

- the geometries of the building stock from the Master Plan of the commune of Renca (AutoCAD file of 2017);
- the energy consumptions in Chile and the characteristics of typical buildings from the Ministry of Energy in 2018 (Ministerio de Energía in Chile, MINEN);
- the Digital Elevation Model of the territory (DEM) from 2011;
- the weather data of 2017 from the Chilean Meteorological Office (Dirección Meteorológica de Chile, DMC).

The result of this data collection was the creation of a uniform, georeferenced database with the building as the basic unit. In fact, data retrieval also consists of the creation of a unique database for all the buildings of Renca, and this work was done through:

- data about the cadaster of housing and population (that is, at census section scale) were associated at the buildings; an example is the number of families or population in each building, which indicates the percentage of occupancy;
- AutoCAD file of the Master Plan of Renca was geolocalized to calculate the geometries and associate the characteristics of the buildings, census sections, and districts in Renca;
- archetype data was gathered and systematically compared with information from the existing built environment to assess their alignment within the commune of Renca;
- the altitude of the terrain was associated at each building using a digital elevation model (DEM);
- the weather stations were geo-localized, and the nearest one with similar altitude was identified to be representative of the local climate conditions.

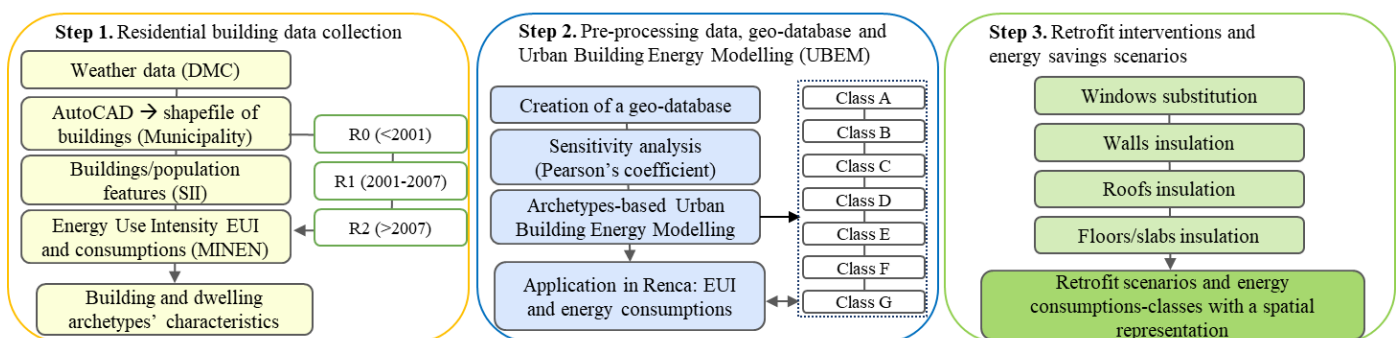


Figure 2. The steps of this analysis including data collection, preprocessing, geodatabase creation, archetype analysis, UBEM, and energy use and energy-saving scenarios in an urban environment.

Step 1 is a crucial part for the outcomes' accuracy of UBEMs because it offers a complete dataset of variables for the buildings. In this work, the year 2017 was selected as a reference considering the availability of the data; besides, 2017 seems to be a year not influenced by anomalous data for energy consumption; more recent data would have been influenced by the pandemic or the next energy crisis. All data, except for the Digital Elevation Model (DEM) from 2011, are aligned with the 2017 timeframe. The DEM, depicting the terrain's elevation, remains relevant as the altitude of the territory does not undergo significant changes over the six-year period.

Step 2. Preprocessing and energy modeling. The geodatabase of the buildings in Renca was completed with the calculation of some energy-related variables using the field calculator of QGIS. Next, the geodatabase was corrected by selecting only residential heated buildings, and the outliers were statistically identified and eliminated. In energy modeling at urban scale, all variables used in the model must be available for all buildings in the city, otherwise the model is not applicable. Using all the information about archetypes, available also at urban scale, a sensitivity analysis was performed to identify the main energy-related variables. For this analysis, Pearson's correlation coefficient R was used, evaluating linear

correlations with the EUIs. Then, an archetype-based UBEM was determined to calculate the EUI for residential buildings.

Therefore, energy modeling was applied to the entire city and categorized accordingly the current residential energy rating classes defined by the Ministry of Housing and Urbanism (Ministerio de Vivienda y Urbanismo MINVU).

Step 3. Identification of energy-saving scenarios by typical retrofitting interventions. The main retrofitting interventions for the eight archetypes were identified with the resulting space-heating energy savings. To calculate the EUI after retrofit interventions, energy savings percentages were applied to the actual EUI by type of building and period of construction. The retrofitting interventions on the building envelope were chosen with the aim of reducing the energy use so that, subsequently, systems that exploit renewable energy sources can be utilized to achieve clean energy transition in cities.

A more detailed description of Step 1 is given in the next paragraph.

Housing Data Collection (Step 1)

To characterize the energy-related features of the existing housing stock, the latest cadaster database by SII was used [58]. This database has recently been available to the public, and it contains relevant georeferenced data of buildings (represented in the QGIS with polygons) and population of the commune of Renca, including the following: type of land use (i.e., residential, commercial, or industrial), footprint area, year of construction, predominant construction type (i.e., brick masonry, timber frame, or concrete), and number and typology of inhabitants and families. For the analysis performed on Renca and district CD-3, only residential uses were taken into account. This resulted in a dataset of 25,100 residential buildings (about 90% in total). All of these data, along with the envelope thermal properties set by MINEN [53], were implemented in the geodatabase using the shapefile of the buildings retrieved from the Municipality of Renca [60]. To generate a 3D model for the entire district, the heights of the buildings, not given in the SII database, were derived by multiplying the number of stories assigned by the municipal cadaster [59,60] with the typical height of dwellings set by the national building codes (approximately 2.3–2.86 m) [53].

The space-heating energy demand of dwellings was taken from studies and questionnaires by MINEN [61]. Representative energy use data of archetypes were obtained from a recent national survey carried out in 2018 on a sample of 3500 households in Chile from different climatic regions and socioeconomic conditions. This study describes the statistical analysis of Chilean dwellings with 95% confidence and maximum error $\pm 5\%$, considering type of building, envelope and technological system characteristics, standard of living of the occupants, user behavior, and energy consumption. As part of this study, eight representative archetypical dwellings were chosen and further in-depth analyses on space-heating energy use and energy-saving potential were carried out.

Table 2 shows the main physical features of the eight Chilean dwelling archetypes [61]. The dwelling archetypes comprise a range of existing houses and apartments built on brick masonry, timber framing, or reinforced concrete. The surface-to-volume ratio, S/V , ranges between 1.00 and 1.32 m^2/m^3 for detached and terrace houses, and 0.11–0.30 m^2/m^3 for intermediate apartments in condominiums with only one external wall. The windows-to-wall ratio is approximately 20% and the windows-to-net-floor-area is 20% too.

Figure 3 illustrates the space-heating energy demand for the entire sample of dwelling archetypes categorized by construction periods: R0, R1, and R2 [61]. For dwellings built before 2001 (period R0), no thermal insulation was used on any envelope element; for those built between 2001 and 2007 (period R1), roof insulation was used to comply with the minimum thermal transmittance U_{roof} of 0.47 $\text{W}/\text{m}^2/\text{K}$; for dwellings built after 2007 (Period R2), additional insulation was used for the external walls to meet a minimum of $U_{\text{wall}} = 1.9 \text{ W}/\text{m}^2/\text{K}$ and for the external floor/slabs to meet a minimum of $U_{\text{floor}} = 0.7 \text{ W}/\text{m}^2/\text{K}$.

Table 2. Typical dwelling and building archetypes.**Type 1.** One-story detached, brick masonry house

total useful area		60.8	m ²
net heated area		56.5	m ²
wall area		83.8	m ²
roof area		60.8	m ²
ceiling height		2.4	m ²
windows area	N-W	5.4	m ²
	N-E	7.8	m ²
	S-W	0.5	m ²
	S-E	4.8	m ²
S/V		1.32	m ² /m ³

Type 2. Two-story detached, brick masonry house

total useful area		123.3	m ²
net heated area		221.2	m ²
wall area		172.2	m ²
roof area		123.3	m ²
ceiling height		2.86	m ²
windows area	N-W	28.7	m ²
	N-E	16.4	m ²
	S-W	0	m ²
	S-E	7.3	m ²
S/V		1.02	m ² /m ³

Type 3. Two-story detached, lightweight timber-frame

total useful area		67.72	m ²
net heated area		103	m ²
wall area		97	m ²
roof area		67.7	m ²
ceiling height		2.4	m ²
windows area	N	10.1	m ²
	S	5.9	m ²
	W	7.7	m ²
	E	0	m ²
S/V		1.26	m ² /m ³

Type 4. Three-story detached, brick masonry house

total useful area		27.94	m ²
net heated area		51.98	m ²
wall area		41.45	m ²
roof area		27.94	m ²
ceiling height		2.4	m ²
windows area	N	3.3	m ²
	S	2.9	m ²
	W	0	m ²
	E	0	m ²
S/V		1.16	m ² /m ³

Table 2. Cont.

Type 5. One story semi-detached, brick masonry house

total useful area		67.42	m ²
net heated area		62.7	m ²
wall area		56.36	m ²
roof area		81.7	m ²
ceiling height		2.4	m ²
windows area	N	3.95	m ²
	S	1.44	m ²
	W	0	m ²
	E	0	m ²
S/V		1.12	m ² /m ³

Type 6. Three-story terrace, brick masonry/timber frame

total useful area		52	m ²
net heated area		84.7	m ²
wall area		41	m ²
roof area		56.5	m ²
ceiling height		2.3	m ²
windows area	N	5.8	m ²
	S	4.7	m ²
	W	1.6	m ²
	E	0	m ²
S/V		1.00	m ² /m ³

Type 7. Single story intermediate apartment, brick masonry.

total useful area		69.25	m ²
net heated area		64.4	m ²
wall area		5.7	m ²
roof area		0	m ²
ceiling height		2.6	m ²
windows area	N	16.3	m ²
	S	0	m ²
	W	0	m ²
	E	0	m ²
S/V		0.11	m ² /m ³

Type 8. Single story intermediate apartment, reinforced Concrete.

total useful area		118	m ²
net heated area		109.7	m ²
wall area		83.8	m ²
roof area		0	m ²
ceiling height		2.6	m ²
windows area	N	12	m ²
	S	9.8	m ²
	W	0	m ²
	E	0	m ²
S/V		0.30	m ² /m ³

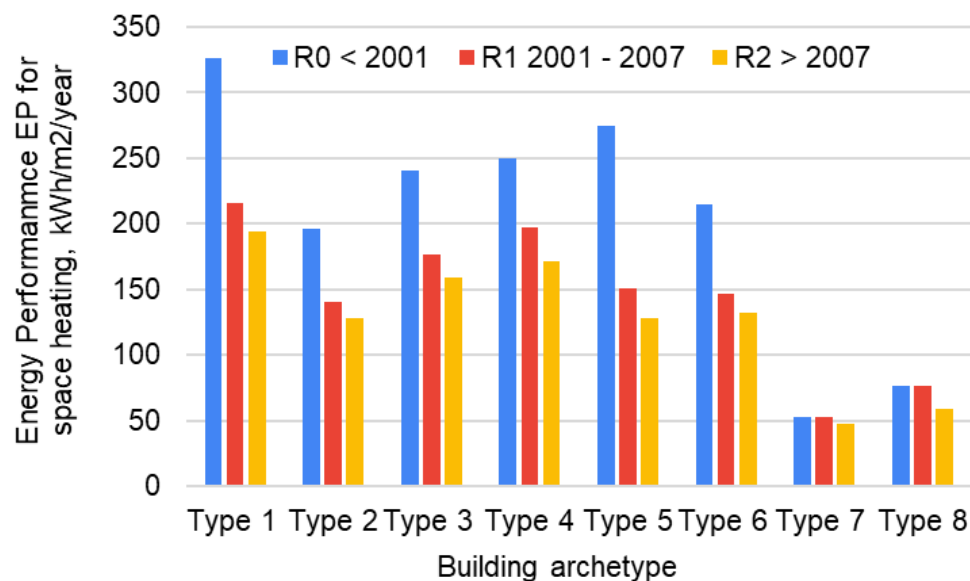


Figure 3. Space-heating energy demand for the eight dwelling archetypes by period of construction (R0, R1, and R2).

The thermal transmittances (U) of typical buildings in the climate zone ZT 3 of Santiago are reported in Table 3. For walls, the value of thermal transmittance depends on the archetype: for archetypes 1, 2, 3, 4, and 6 with brick walls, U_{wall} is $2.3 \text{ W/m}^2/\text{K}$; for archetype 5, with a wooden structure, U_{wall} is $2.7 \text{ W/m}^2/\text{K}$; for apartments of archetypes 7 and 8, U_{wall} is $3.4 \text{ W/m}^2/\text{K}$.

Table 3. Thermal transmittances of archetypes by period of construction in climate zone ZT 3.

Period of Construction	U_{glass}	U_{wall}	U_{roof}	U_{floor}
	$\text{W/m}^2/\text{K}$			
R0	5.8	2.3–3.4	3.2	1.4
R1	5.8	2.3–3.4	0.47	1.4
R3	5.8	1.9	0.47	0.7

It can be observed that there is a large difference in the annual space-heating energy performance index EP for:

- different S/V values: the type 7 dwellings (with the lowest S/V ratio) and type 1 dwellings (with the highest S/V ratio) have an energy performance that varies between 50 and over $300 \text{ kWh/m}^2/\text{year}$;
- different periods of construction (R0, R1, and R2): old buildings (i.e., R0) have a higher energy performance index; the EP is reduced by 20–30% from period R0 to R1 and by 3–10% from period R1 to R2;
- for the intermediate-floor apartments (types 7 and 8), energy-use changes only from period R1 to R2 because the walls represent the only heat-loss surfaces.

4. Results

The use of QGIS allows the use of a geo-package to manage the data collection and preprocessing phases more easily for building energy modeling on an urban scale with a place-based approach. The database manager (DB manager) plugin allows application of the queries to quickly calculate each energy-related variable, even with a standard personal computer.

4.1. Energy Modeling from Building Archetypes (Step 2)

After the data collection and preprocessing phases, a complete geo-package was created to allow the evaluation and application of an archetype-based UBEM for the commune of Renca.

A sensitivity analysis with Pearson's coefficient R of the data and EUI regarding archetypes allowed identification of the main energy-related variables: the period of construction and the surface-to-volume ratio S/V with $R = -0.93$ and 0.96 , respectively. This result was expected [62] because, thanks to energy-saving laws, the construction period indicates the characteristics of the envelope components of the buildings. The S/V also influences energy consumption because it indicates the non-compactness of a building and therefore the quantity of surfaces that disperse heat towards the external or unheated environments.

To estimate the space-heating energy demand of dwellings at the urban level, the EUI of each archetype was calculated, taking into account the respective S/V ratio by period of construction and the heated volume (in Figure 4). As depicted in the graph on Figure 4, linear regression equations were generated for the sample of archetypes in each regulatory period, attaining good coefficients of determination: 0.93 (period R0) and 0.92 (periods R1 and R2).

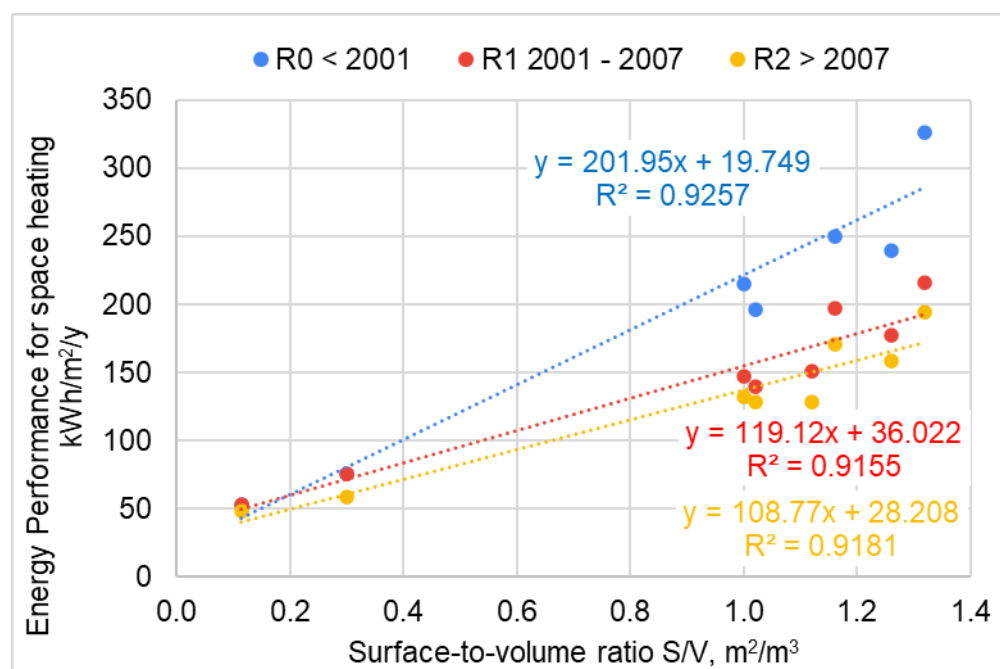


Figure 4. The relationship between surface-to-volume ratio of dwellings and space-heating energy use.

These equations were applied to the building stock considering the characteristics of each building in Renca to evaluate the spatial distribution of energy performance for space heating.

In turn, the 3D model of the built environment compiled with QGIS was used to map the distribution of the characteristics of residential buildings (i.e., period of construction, S/V , and percentage of occupied dwellings) across the entire city. The resulting map plotted in Figure 5 is consistent with the three main residential areas of the district, which can be clearly recognized as follows:

- a low-rise residential area of one-story single-family houses with S/V ratio higher than $1.09 m^2/m^3$ (39.7%),
- terrace houses with two floors with an $S/V = 0.9 - 1.09 m^2/m^3$ (30.0%),
- little condominiums of 3–4 floors with an S/V of $0.6-0.9 m^2/m^3$ (21.5%).



Figure 5. The surface-to-volume ratio S/V of residential buildings in Renca, m^2/m^3 .

Large condominiums with more than four floors account only for the 8.8% of the buildings with an S/V lower than $0.6 m^2/m^3$.

As can be observed, district CD-3 is a more homogeneous district, with a low-rise residential area with detached (57.3%) and terrace (34.9%) houses, and only few condominiums in the newer area of CZ-2.

By implementing the equations in Figure 4 given for each regulatory period of R0, R1, and R2 on the buildings' geo-package, the energy performance and energy class of the entire housing stock was modelled (in Figure 6).



Figure 6. The energy classes of residential buildings in Renca according to Chilean climate zone 3.

The results, plotted in Figure 6, are categorized according to the Chilean energy classes (in Table 4) that were calculated knowing the energy performance index $EP_{nd,H}$ kWh/m²/year resulting from the archetype and GIS-based UBEM. In Renca, the most frequent energy class is E at 83.6% because almost all buildings are old, detached houses with a S/V from 1.09 and 1.2 m²/m³. It can be observed that some areas are in class G; these are mainly new buildings, where $EP_{nd,H} \geq 149$ kWh/m²/y (instead of $EP_{nd,H} \geq 362$ kWh/m²/y for old buildings). Also, in district CD-3, some new buildings are in class G, while classes D, C, B, and A are more compact, old buildings with a low S/V ratio (in Figure 5).

Table 4. Building energy performance classification $EP_{nd,H}$ (kWh/m²/year for space-heating demand) by period of construction in Chilean climate zone ZT 3.

Energy Classes	Period of Construction			
	Reference Building	268 kWh/m ² /y	159 kWh/m ² /y	111 kWh/m ² /y
(energy saving % compared with reference building)		R0 <2001	R1 2001–2007	R2 >2007
A (>60%)		$EP_{nd,H} < 107$	$EP_{nd,H} < 64$	$EP_{nd,H} < 44$
B (50/60%)		$107 \leq EP_{nd,H} < 134$	$64 \leq EP_{nd,H} < 80$	$44 \leq EP_{nd,H} < 56$
C (35/50%)		$134 \leq EP_{nd,H} < 174$	$80 \leq EP_{nd,H} < 103$	$56 \leq EP_{nd,H} < 72$
D (15/35%)		$174 \leq EP_{nd,H} < 228$	$103 \leq EP_{nd,H} < 135$	$72 \leq EP_{nd,H} < 94$
E (−10/15%)		$228 \leq EP_{nd,H} < 295$	$135 \leq EP_{nd,H} < 175$	$94 \leq EP_{nd,H} < 122$
F (−35/−10%)		$295 \leq EP_{nd,H} < 362$	$175 \leq EP_{nd,H} < 215$	$122 \leq EP_{nd,H} < 149$
G (<−35%)		$EP_{nd,H} \geq 362$	$EP_{nd,H} \geq 215$	$EP_{nd,H} \geq 149$

4.2. Retrofitting Interventions (Step 3)

In order to study retrofitting interventions, the conditions of the original buildings were analyzed. Almost all residential buildings were built before 2001, in period R0, meaning that these buildings were built without energy-savings regulations (83% in Table 5); therefore, they have no thermal insulation nor other energy-efficiency measures. Only a few buildings belong to the R2 period of construction, and these buildings have insulated roofs (from 2001 onward), walls and floors (from 2007 onward); this means they have lower heat dispersion and good energy efficiency levels. Table 5 shows the percentage of buildings in Renca and in the old district of CD-3 according to different periods of construction. As can be observed, old buildings that are not insulated represent the majority (in the R0 period of construction) and this indicates that an improvement in terms of energy saving can be promising.

Table 5. Percentage of buildings by period of construction.

Building Location	R0 < 2001	R1 2001–2007	R2 > 2007
Renca	83.0%	6.4%	10.6%
CD-3 district	94.8%	0%	5.2%

In Chile, there are four main retrofitting interventions for residential buildings [61]:

- window replacement: existing windows are replaced with PVC casements and double-glazed windows ($U = 1.1$ W/m²/K);
- wall insulation: additional thermal insulation is installed on the outside of existing walls with a thickness of 20 cm;
- roof insulation: additional thermal insulation is installed on the inside of roofs with a thickness of 15 cm;

- floor insulation: additional thermal insulation is installed on the inferior slab/floor with a thickness of 1 cm.

The EUI after these four retrofitting measures were simulated applying energy savings percentages to the UBEM by type of building and period of construction, considering the feasibility of the measures. Table 6 shows the percentage energy savings by period of construction for the main four retrofitting measures [61]. Then, with the QGIS, the percentage energy savings were implemented for each building to evaluate the energy savings after the four retrofitting interventions (in Table 7). Analyzing the percentages of energy savings, it becomes evident that substituting roofs, walls, and windows yields more substantial benefits compared to slab insulation, which exhibits minimal impact. Roof insulation has low values of energy savings in newer buildings because Chilean laws already partially require this insulation measure.

Table 6. Energy savings following the main retrofitting interventions by the period of construction of buildings.

Retrofitting Interventions	Energy Savings			
	Period of Construction:	R0 < 2001	R1 2001–2007	R2 > 2007
1. Window substitution ($U = 1.1 \text{ W/m}^2/\text{K}$)		14.5%	18.5%	22%
2. Wall thermal insulation, 20 cm		36.5%	50%	46%
3. Roof thermal insulation, 15 cm		32%	5.5%	4.5%
4. Slab thermal insulation, 1 cm		2%	3%	4%

Table 7. Energy savings after the retrofitting measures.

MWh/Year	1. Windows	2. Walls	3. Roofs	4. Slabs
Saved energy demand	173,079	428,922	324,048	24,778

Figure 7 shows the energy performance after retrofitting interventions for the district of CD-3. Before retrofitting, the main energy class was class E. After windows were substituted this became class D (Figure 7a); however, new buildings (with a period of construction of R2) that were in class G before retrofitting, became class E and F after intervention (in orange and red). The energy classes were also improved after roof insulation (in Figure 7b), with only a little progress for new buildings that remained in classes F and G because the roofs were already insulated.



Figure 7. Energy classes after retrofitting interventions in district CD-3: (a) window substitution; (b) thermal insulation of roofs.

In assessing economic advantages, the payback time serves as a valuable metric, taking into account both the retrofitting intervention costs and the annual economic savings.

The cost of the retrofitting measures was evaluated considering materials and labor costs in Chile; data for 2019 were considered, as they were not influenced by the COVID-19 pandemic, the Ukrainian war, or the subsequent the energy crisis (in Table 8).

Table 8. Four retrofitting interventions: costs, renovation areas, and consumption savings.

Retrofitting Intervention	1. Windows	2. Walls	3. Roofs	4. Floors
Intervention costs (\$/m ²)	216	120	105	80
Retrofitted surfaces (m ²)	713,841.7	4,199,068.8	4,597,772.1	4,597,772.1
Cost of interventions (k\$)	154,189,807	503,888,256	482,766,071	367,821,768
Consumption savings (MWh/year)	262,241,078	649,882,103	490,982,481	53,701,209

The calculation of the annual economic savings for each building and for each retrofit intervention, requires knowledge of energy demand, average heating system efficiency, and price of energy:

- the actual energy demand was calculated multiplying the EUI (from the equations in Figure 4) by the net heated area and the percentage of occupancy;
- the actual energy consumption was calculated dividing the energy demand by the average efficiency of the space-heating systems, that is 66% (in Table 9);
- the energy savings was calculated multiplying the energy consumption by the percentage energy savings reported in Table 6 evaluated by archetype;
- the cost of retrofit interventions was evaluated multiplying the cost per unit of area (in Table 8) by the area to be retrofitted;
- the economic savings were evaluated multiplying the energy savings by the average price of fuels for residential buildings, that is 0.106 USD/kWh (from Table 9).

Table 9. Energy source, prices, and GHG emissions by fuel for households in Chile.

Fuel	Households (%)	System Efficiency (%)	Price of Energy (USD/kWh)	GHG Emissions (kgCO _{2eq} /kWh)
Liquefied petroleum gas	40.3	65	0.110	0.254
Kerosene	35.6	60	0.104	0.270
Firewood	12.2	55	0.054	0.395
Electricity	11.4	100	0.154	0.480
Natural Gas	0.3	70	0.086	0.252
Others	0.2	70	0.102	0.330

Utilizing the information from Tables 8 and 9, calculations were performed for energy prices and economic savings across the entire commune of Renca. Additionally, the average reduction in greenhouse gas (GHG) emissions was determined, considering the GHG emissions categorized by fuel type as presented in Table 9 (i.e., MINEN [53] and MINVU [63]).

This result was compared with simple payback time to define an effective energy policy in Renca, considering not only economic benefits but also environmental impact with the reduction in GHG emissions, which is a priority in Santiago area.

The economic savings after the four interventions were compared with payback time and GHG emissions (in Table 10 and Figure 8). Considerable outcomes in economic savings

and greenhouse gas emission reduction are achieved through wall and roof insulation. Window substitution, characterized by smaller surfaces, is cost-effective with a competitive payback time. In contrast, thermal insulation for the inferior slab or floor yields relatively modest energy savings compared to other retrofitting interventions, resulting in a longer payback time.

Table 10. Economic benefits of retrofitting interventions on buildings in Renca.

	1. Windows	2. Walls	3. Roofs	4. Floors/Slabs
Economic savings (k\$/year)	27,787,065	68,861,508	52,024,504	5,690,180
Simple payback time (year)	5.55	7.32	9.28	64.64
GHG reduction (kgCO _{2,eq})	79,408,696	196,789,450	148,673,423	16,261,156

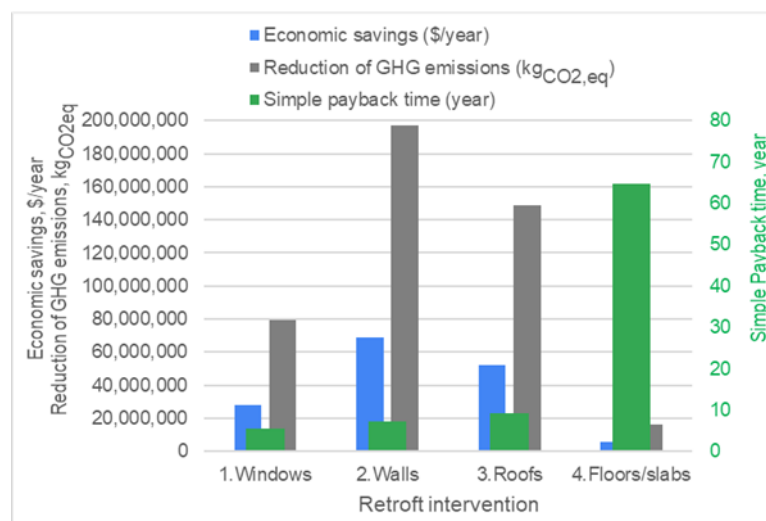


Figure 8. Main economic and environmental results of retrofitting interventions: economic and GHG emission savings and simple payback time.

5. Discussion

The results of the urban modeling analysis undertaken for Renca so far show that with minor low-cost interventions to the existing fabric of housing stock, significant economies of scale can be achieved in terms of reducing space-heating energy demands and running energy costs.

The bar chart in Figure 8 shows the payback time is an economic analysis that compares the cost of an intervention with its benefits, the ratio of costs to the annual economic savings. Window substitution and the thermal insulation of walls and roofs are economically sustainable, while floor insulation has a payback time of 60 years. The latter does not appear to be in line with the action plan for the sustainable development of buildings in Chile, but it can be an additional measure to further reduce energy consumption in cities, facilitating effective use of RES and improving thermo-hygrometric comfort inside homes.

The amount of GHG emissions was used to measure the environmental impact of energy use and the air quality load for space-heating. In Figure 8, the GHG emissions saved through different interventions are represented and, because of the high use of fossil fuels, the bar chart shows that they depend directly on energy savings. A large reduction in GHG emissions results from interventions on walls and roofs, representing a reduction of three and two times that of the window intervention, respectively; floor interventions were associated with less of a reduction in GHG emissions.

To conclude, if it is necessary to reduce energy consumption in the Santiago area for energy production from renewable sources to be effective; the priority renovation interventions are the insulation of walls and roofs. However, replacing windows and insulating floors are also important to further reduce energy consumption, given that the availability of renewable resources is reduced in cities.

5.1. Policy Suggestions

According to the World Energy Council, the level of sustainability of an energy system can be measured through three indicators [64]: energy security, environmental sustainability, and energy equity (accessibility and affordability). Chile has the highest indicators in Latin America before Argentina and Brazil. Energy security is increasing due to a good mix of energy sources and a higher use of coal to produce electricity; for the same reason and in terms of the increase of energy use in the transport sector, environmental sustainability is decreasing. Energy equity is quite stable and, only recently, has been decreasing due to the higher prices of energy amid the global energy crisis.

In 2022, a new government began to work in Chile and the National Energy Policy, Energy Efficiency Law, and National Energy plans were promulgated to reach the carbon-neutral target and be resilient to climate change in 2050. In the short–medium term, the aim is to reduce energy intensity by 10%, to increase the use of wind and solar sources, and to reduce the price of energy. The 10% of EUI reduction for residential buildings could be obtained with window substitution, which is the easier retrofit measure.

In Figure 9, the primary energy consumption of Chile, Argentina, and Brazil are compared [65]. Chile has half the consumption of Argentina and 13% of that of Brazil; however, the consumption per person (in orange) is higher, especially comparing Chile with Brazil, representing +146%. Chile is more similar to countries such as Portugal and Hungary in terms of consumption per person. The energy consumption per person can be reduced with environmental and economic improvements.

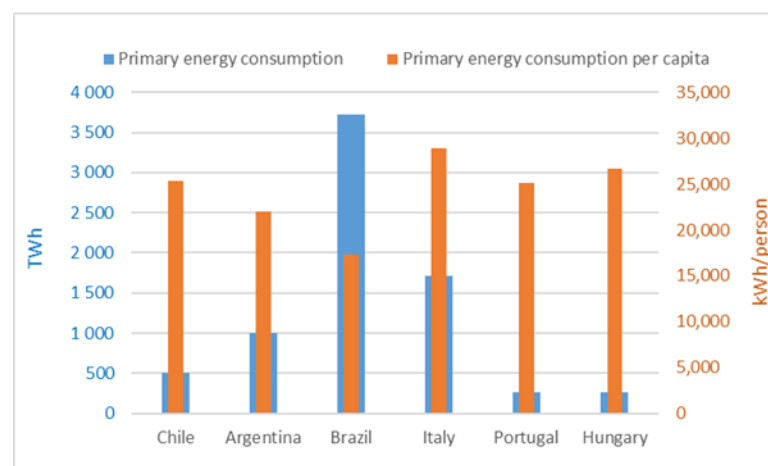


Figure 9. Comparison of primary energy consumption of Chile and some other countries.

According to this revision, the main measures that can be implemented in the building sector, to be carbon neutral in 2050, are energy efficiency measures and more clean energy sources, especially solar technologies and heat pumps. Furthermore, the use of smart networks and grids in cities could improve the storage and share of energy to better boost renewable resources.

5.1.1. Saving Energy with Energy Efficiency Measures

The cleanest energy is the one that is not consumed, so priority should be given to energy conservation. For many decades, there have been available technologies that could be used to reduce energy consumption in buildings, comprising thermal insulation for

exposed walls, roofs, and floors, or the replacement of windows. These passive building retrofitting measures are a priority for reducing consumption. Then, systems with lower power will be installed and perhaps associated with renewables.

Indeed, retrofitting interventions on technological systems can reduce energy consumption, too, including those requiring only a small amount of retrofit labors; for example, the use of condensing boilers, low-temperature emission systems, climate probes, and the installation of control systems in each thermal zone of the building. These measures are easy to install, have low costs, and economic incentives can accelerate the promotion of these interventions.

At the district/urban level, the use of systems/plants with a high energy conversion rate can reduce the economic pressure of energy bills and the amount of GHG emissions. The use of a combined heat and power plants is a good example of a high-efficiency system: it produces electricity and uses a quota of the heat lost to distribute hot water with district heating networks. As Chile is a narrow country along the west coast of South America, energy transportation (electricity and heat) is a problem; so, energy should be produced with efficient systems where it is used.

5.1.2. Use of RES and Solar Technologies

Chile is a rich country for renewable energy sources, especially solar and wind. One of the key actions for energy transition is the increase in penetration of renewable energy sources to improve the mix of different energy types towards more electrification of systems and more storage.

The metropolitan area of Santiago de Chile is located between the coast and the mountains, and the wind can only be exploited along the coast. Therefore, in Santiago, the main renewable source available is the sun, owing to the strong solar irradiation. With mainly detached buildings with one or two families and a high roof area per family, active roofs with photovoltaic panels and solar thermal collectors are the best solution to reach high percentages of self-consumption and self-sufficiency for domestic hot water and electricity consumption; solar technologies with a thermal storage system and batteries are the optimal solution for this area of Chile.

5.1.3. People's Awareness and Smart Technologies

The awareness of the use of energy is fundamental, especially with a renewable mix of energy sources that follow seasonal and daily behaviors. The low energy demand of efficient buildings can be supplied by the available renewable sources only if the use of energy is managed and controlled with smart technologies. This limit in the use of energy is overcome by the advantages associated with the reduction in energy costs and the lower environmental impact of energy use.

The use of energy can also join users, producers, and prosumers to create a community of citizens or a renewable energy community with the aim of producing, distributing, and sharing energy with benefits for all. The overproduction of energy of a prosumer can be stored or shared with other members and vice versa when there is an uncovered demand. Smart grids and networks can manage and optimize the energy fluxes to save money and reduce GHG emissions. This behavior increases the instantaneous self-consumption and self-sufficiency of the community, reducing energy dependence and the risk of blackout.

The emphasis on creating a low-carbon community extends beyond civil energy to encompass various sectors, including transportation. Sustainable alternatives such as bicycles, electric scooters, and electric vehicles play a crucial role in fostering a clean-energy approach within communities.

5.1.4. Energy and Climate Policies

The level of energy efficiency in buildings can be regulated by laws, standards, and building codes. The energy efficiency of buildings in a city considers the type of building stock, the socioeconomic state of population, costs and payback time of technologies, price

of energy, climatic conditions, availability of renewable energy sources, actual energy systems, and climate targets set by local, national, and international agreements.

Incentives to push the realization of energy efficiency measures include the following:

- economic incentives that are provided to reduce the costs of the technologies to be installed;
- tax deductions for the expenditure of energy efficiency interventions or renewable technologies;
- economic incentives on clean energy production, mainly used for electrical energy produced by grid-connected photovoltaic systems;
- economic incentives on sharing energy between members of a community, mainly used for electrical energy;
- discounts on urbanization costs for new projects that have higher energy efficiency level compared with the energy requirements of standards;
- volumetric bonuses in derogation of urban plans for measures that have higher energy efficiency compared with the energy requirements of standards.

The selection of the type of incentive can accelerate energy transition by trying to implement all of the interventions aimed at reducing the consumption of energy produced from fossils fuels.

6. Conclusions

The methods and tools applied in this study have allowed a path to be recognized to move towards modeling building energy performance on an urban scale with limited available spatial and energy consumption data. This is particularly relevant for urban planners and decision-makers in low-income municipalities where the relationship between the performance of the urban fabric and household energy consumption is still not well understood. The proposed archetype- and GIS-based UBEM provides criteria and strategic interventions requiring a small amount of investment and with payback being achieved over a short period of time, to contribute to a reduction in energy demands. For further studies to be performed, an overview of the methods applied in this study is given below.

Urban building energy modeling was performed considering the EUI of eight archetypes, representing the most common types of building in Chile. The UBEM was developed considering linear regression of the main energy-related variables, namely, gross volume, surface-to-volume ratio, the period of construction, and occupancy level. The utilization of a GIS-based assessment facilitated the incorporation of real features specific to each building, enabling the application of EUI through archetype-based UBEM. The geo-database of building stock reveals a predominant presence of detached houses housing one or two families, constructed before 2001, characterized by the absence of insulation and low-efficiency technological systems in residential buildings. In this context, it is necessary to intervene with energy efficiency measures, and the margins for improvement are promising. The application of the archetype based UBEM with GIS on the buildings of Renca also describes the spatial distribution of energy consumption and energy classes.

Then, the percentage of energy savings and the costs of four main retrofitting measures on the envelope of the buildings were applied to the residential buildings to evaluate the new consumption, resulting energy savings, payback times of the interventions, and reduction in GHG emissions. In Chile, the more convenient retrofitting intervention is wall insulation, followed by roof insulation, window substitution, and then floor/slab insulation. The aim of this study was to evaluate the possible energy and climate targets considering the real characteristics of the building stock.

The annual energy savings from the insulation of walls is 650 GWh/year with a payback time of only 7 years, and a reduction in GHG emissions is 200,000 tCO₂/year. This investment in energy saving, together with the other interventions, will generate benefits not only for 7 years, but for the entire life of the buildings, and provide relative environmental and economic benefits. Moreover, the installation of solar thermal collectors and photovoltaic modules could be implemented along with the roof insulation. These

results depend on the type of urban environment in Renca with low-rise single-family buildings and how the energy is utilized. This analysis was carried out using Renca, in the central area of Chile, as the research area. However, the same archetype- and GIS-based methodology can be easily replicated for other Chilean cities or in other countries. In addition, the resulting spatial distribution of data will be used to verify the implementation of sustainable energy systems, for example, with renewable solar technologies, heat pumps, and district heating networks with a CHP plant to supply electricity and heat with higher efficiencies, lower costs, and GHG emissions, and subsequently, increasing energy security, environmental sustainability, and energy equity.

Finally, the strength and opportunity of this type of modeling is based on the possibility of using data available from urban studies and plans and, depending on these data, the type of UBEM can be chosen. In this case, an archetype- and GIS-based UBEM was selected due to the lack of consumption data, the availability of eight archetypes, and thanks to the possibility of creating a geodatabase with information on the actual buildings and population. This type of model is very easy to use, is flexible, and requires short simulation times. The weaknesses and threats are related to the availability of data, their accuracy, and the ability to manage large quantities of data, a geodatabase or geopackage, and the QGIS tools. Usually, the data collection and preprocessing are the main time-consuming phases.

Author Contributions: Conceptualization, G.M.; methodology, G.M.; software, M.A., Y.H. and Z.X.; validation, G.M.; resources, G.F. and G.M.; writing—original draft preparation, G.M., Y.H., Z.X. and G.F.; writing—review and editing, G.M.; supervision, G.M. All authors have read and agreed to the published version of the manuscript.

Funding: This research received no external funding.

Data Availability Statement: Data can be shared on request.

Conflicts of Interest: The authors declare no conflicts of interest.

References

1. IEA World Energy Outlook. 2021. Available online: <https://www.iea.org/topics/world-energy-outlook> (accessed on 12 September 2022).
2. Liddell, C. Fuel poverty comes of age: Commemorating 21 years of research and policy. *Energy Policy* **2012**, *49*, 2–5. [CrossRef]
3. Heindl, P. Measuring fuel poverty: General considerations and application to German household data. *FinanzArchiv/Public Financ. Anal.* **2015**, *71*, 178–215. [CrossRef]
4. Charlier, D.; Legendre, B. Fuel poverty in industrialized countries: Definition, measures and policy implications a review. *Energy* **2021**, *236*, 121557. [CrossRef]
5. Sy, S.A.; Mokaddem, L. Energy poverty in developing countries: A review of the concept and its measurements. *Energy Res. Soc. Sci.* **2022**, *89*, 102562. [CrossRef]
6. Urquiza, A.; Amigo, C.; Billi, M.; Calvo, R.; Labraña, J.; Oyarzún, T.; Valencia, F. Quality as a hidden dimension of energy poverty in middle-development countries. Literature review and case study from Chile. *Energy Build.* **2019**, *204*, 109463. [CrossRef]
7. Nussbaumer, P.; Nerini, F.F.; Onyeji, I.; Howells, M. Global Insights Based on the Multidimensional Energy Poverty Index (MEPI). *Sustainability* **2013**, *5*, 2060–2076. [CrossRef]
8. Bouzarovski, S.; Petrova, S. A global perspective on domestic energy deprivation: Overcoming the energy poverty–fuel poverty binary. *Energy Res. Soc. Sci.* **2015**, *10*, 31–40. [CrossRef]
9. Boardman, B. *Fixing Fuel Poverty: Challenges and Solutions*; Earthscan: Londres, UK, 2010.
10. Fuller, S.; Barber, L.B.; Mah, D.N.-Y. Narratives of energy poverty in Hong Kong. *Energy Build.* **2019**, *191*, 52–58. [CrossRef]
11. Esily, R.R.; Yuaning, C.; Ibrahim, D.M.; Houssam, N.; Makled, R.A.; Chen, Y. Environmental benefits of energy poverty alleviation, renewable resources, and urbanization in North Africa. *Util. Policy* **2023**, *82*, 101561. [CrossRef]
12. Thomson, H.; Day, R.; Ricalde, K.; Brand-Correa, L.I.; Cedano, K.; Martinez, M.; Santillán, O.; Delgado Triana, Y.; Luis Cordova, J.G.; Milian Gómez, J.F.; et al. Understanding, Recognizing, and Sharing Energy Poverty Knowledge and Gaps in Latin America and the Caribbean—Because Conocer Es Resolver. *Energy Res. Soc. Sci.* **2022**, *87*, 102475. [CrossRef]
13. Encinas, F.; Truffello, R.; Aguirre-Nuñez, C.; Puig, I.; Vergara-Perucich, F.; Freed, C.; Rodríguez, B. Mapping Energy Poverty: How Much Impact Do Socioeconomic, Urban and Climatic Variables Have at a Territorial Scale? *Land* **2022**, *11*, 1449. [CrossRef]
14. Plominsky, G.F.; Arias, A.M.; Rivera, M.I.; Zepeda-Gil, C. Pobreza energética en contextos de exclusión urbana: Nuevos enfoques para la acción desde América Latina. *Rev. INVI* **2023**, *38*, 1–16. [CrossRef]
15. Wang, H.; Maruejols, L.; Yu, X. Predicting energy poverty with combinations of remote-sensing and socioeconomic survey data in India: Evidence from machine learning. *Energy Econ.* **2021**, *102*, 105510. [CrossRef]

16. Nathan, H.S.K.; Hari, L. Towards a new approach in measuring energy poverty: Household level analysis of urban India. *Energy Policy* **2020**, *140*, 111397. [CrossRef]
17. Reyes, R.; Schueftan, A.; Ruiz, C.; González, A.D. Controlling air pollution in a context of high energy poverty levels in southern Chile: Clean air but colder houses? *Energy Policy* **2019**, *124*, 301–311. [CrossRef]
18. Molina, C.; Toro A, T.; Morales S, R.G.; Manzano, C.; Leiva-Guzmán, M.A. Particulate matter in urban areas of south-central Chile exceeds air quality standards. *Air Qual. Atmos. Health* **2017**, *10*, 653–667. [CrossRef]
19. Pérez-Fargallo, A.; Leyton-Vergara, M.; Wegertseeder, P.; Castaño-Rosa, R. Energy Poverty Evaluation Using a Three-Dimensional and Territorial Indicator: A Case Study in Chile. *Buildings* **2022**, *12*, 1125. [CrossRef]
20. Li, S.; Meng, J.; Zheng, H.; Zhang, N.; Huo, J.; Li, Y.; Guan, D. The driving forces behind the change in energy consumption in developing countries. *Environ. Res. Lett.* **2021**, *16*, 054002. [CrossRef]
21. AA.VV. *Balance Energético (1992–2022)*; Ministerio de Energía (MINEN), Gobierno de Chile: Santiago, Chile, 2023. Available online: <https://energia.gob.cl/pelp/balance-nacional-de-energia> (accessed on 20 July 2023).
22. AA.VV. *Manual de Aplicación Reglamentación Térmica*; Ministerio de Vivienda y Urbanismo (MINVU), Gobierno de Chile: Santiago, Chile, 2006.
23. Jorquera, H.; Barraza, F.; Heyer, J.; Valdivia, G.; Schiappacasse, L.N.; Montoya, L.D. Indoor PM2.5 in an urban zone with heavy wood smoke pollution: The case of Temuco, Chile. *Environ. Pollut.* **2018**, *236*, 477–487. [CrossRef]
24. Prieto-Parra, L.; Yohannessen, K.; Brea, C.; Vidal, D.; Ubilla, C.A.; Ruiz-Rudolph, P. Air pollution, PM 2.5 composition, source factors, and respiratory symptoms in asthmatic and nonasthmatic children in Santiago, Chile. *Environ. Int.* **2017**, *101*, 190–200. [CrossRef] [PubMed]
25. Díaz-Robles, L.A.; Fu, J.S.; Vergara-Fernández, A.; Etcharren, P.; Schiappacasse, L.N.; Reed, G.D.; Silva, M.P. Health risks caused by short term exposure to ultrafine particles generated by residential wood combustion: A case study of Temuco, Chile. *Environ. Int.* **2014**, *66*, 174–181. [CrossRef] [PubMed]
26. AA.VV. *Planes de Descontaminación Atmosférica: Guías, Reglamentos y Normativas*; Ministerio del Medio Ambiente (MMA), Gobierno de Chile: Santiago, Chile, 2023.
27. AA.VV. *Tercer Informe Bienal de Actualización de Chile Sobre El Cambio Climático*; Ministerio del Medio Ambiente (MMA), Gobierno de Chile: Santiago, Chile, 2018.
28. Sudhira, H.S.; Ramachandra, T.V.; Jagadish, K.S. Urban sprawl: Metrics, dynamics and modelling using GIS. *Int. J. Appl. Earth Obs. Geoinform.* **2004**, *5*, 29–39. [CrossRef]
29. Deng, Z.; Chen, Y.; Yang, J.; Chen, Z. Archetype identification and urban building energy modeling for city-scale buildings based on GIS datasets. *Build. Simul.* **2022**, *15*, 1547–1559. [CrossRef]
30. Dong, J.; Schwartz, Y.; Mavrogianni, A.; Korolija, I.; Mumovic, D. A review of approaches and applications in building stock energy and indoor environment modelling. *Build. Serv. Eng. Res. Technol.* **2023**, *44*, 333–354. [CrossRef]
31. Borges, P.; Travasset-Baro, O.; Pages-Ramon, A. Hybrid approach to representative building archetypes development for urban models—A case study in Andorra. *Build. Environ.* **2022**, *215*, 108958. [CrossRef]
32. Cooper, J.; Foster, S.; Dias, J.; Mason, E. Review of Social Housing Archetypes to Support EESSH2 Review, 2023, 10.7488/era/3650. Available online: <https://www.climatechange.org.uk/media/5888/cxc-review-of-social-housing-archetypes-to-support-eessh2-february-2023.pdf> (accessed on 20 July 2023).
33. Residential Archotyping for Energy Efficiency Programs. A Guide for Canadian Municipalities. 2022. Available online: <https://www.cleanairpartnership.org/wp-content/uploads/2023/01/Archotyping-Guide-For-Energy-Efficiency-Programs-1.pdf> (accessed on 20 July 2023).
34. Mehta, K.; Zörner, W. Cracking the code: Mapping residential building energy performance in rural Central Asia through building typologies. *SN Appl. Sci.* **2023**, *5*, 349. [CrossRef]
35. Vaisi, S.; Mohammadi, S.; Habibi, K. Heat Mapping, a Method for Enhancing the Sustainability of the Smart District Heat Networks. *Energies* **2021**, *14*, 5462. [CrossRef]
36. Goy, S.; Maréchal, F.; Finn, D. Data for Urban Scale Building Energy Modelling: Assessing Impacts and Overcoming Availability Challenges. *Energies* **2020**, *13*, 4244. [CrossRef]
37. Pasichnyi, O.; Wallin, J.; Kordas, O. Data-driven building archetypes for urban building energy modelling. *Energy* **2019**, *181*, 360–377. [CrossRef]
38. Ang, Y.Q.; Berzolla, Z.; Reinhart, C. Smart meter-based archetypes for socioeconomically sensitive urban building energy modeling. *Build. Environ.* **2023**, *246*, 110991. [CrossRef]
39. Ferrando, M.; Ferroni, S.; Pelle, M.; Tatti, A.; Erba, S.; Shi, X.; Causone, F. UBEM’s archetypes improvement via data-driven occupant-related schedules randomly distributed and their impact assessment. *Sustain. Cities Soc.* **2022**, *87*, 104164. [CrossRef]
40. Ali, U.; Bano, S.; Shamsi, M.H.; Sood, D.; Hoare, C.; Zuo, W.; Hewitt, N.; O’Donnell, J. Urban building energy performance prediction and retrofit analysis using data-driven machine learning approach. *Energy Build.* **2024**, *303*, 113768. [CrossRef]
41. Pongelli, A.; Priore, Y.D.; Bacher, J.-P.; Jusselme, T. Definition of Building Archetypes Based on the Swiss Energy Performance Certificates Database. *Buildings* **2022**, *13*, 40. [CrossRef]
42. Mutani, G.; Alehasin, M.; Usta, Y.; Fiermonte, F.; Mariano, A. Statistical Building Energy Model from Data Collection, Place-Based Assessment to Sustainable Scenarios for the City of Milan. *Sustainability* **2023**, *15*, 14921. [CrossRef]

43. Ballarini, I.; Corgnati, S.P.; Corrado, V. Use of reference buildings to assess the energy saving potentials of the residential building stock: The experience of TABULA project. *Energy Policy* **2014**, *68*, 273–284. [[CrossRef](#)]
44. Ferguson ARA. Housing Models for Use with the Housing Technology Assessment Platform. 2019. Available online: <https://github.com/NRCan-IETS-CE-O-HBC/HTAP-archetypes> (accessed on 8 July 2023).
45. Osman, M.; Saad, M.M.; Ouf, M.; Eicker, U. From buildings to cities: How household demographics shape demand response and energy consumption. *Appl. Energy* **2024**, *356*, 122359. [[CrossRef](#)]
46. Alasmar, R.; Schwartz, Y.; Burman, E. Evaluation of Energy Performance of The Most Prevalent Housing Archetypes in Jordan, CIBSE Technical Symposium, UK April 2022. Available online: <https://www.cibse.org/knowledge-research/knowledge-portal/evaluation-of-energy-performance-of-the-most-prevalent-housing-archetypes> (accessed on 8 July 2023).
47. Cerezo, C.; Sokol, J.; AlKhaled, S.; Reinhart, C.; Al-Mumin, A.; Hajiah, A. Comparison of four building archetype characterization methods in urban building energy modeling (UBEM): A residential case study in Kuwait City. *Energy Build.* **2017**, *154*, 321–334. [[CrossRef](#)]
48. Mutani, G.; Todeschi, V. GIS-based urban energy modelling and energy efficiency scenarios using the energy performance certificate database. *Energy Effic.* **2021**, *14*, 47. [[CrossRef](#)]
49. Rosser, J.F.; Long, G.; Zakhary, S.; Boyd, D.S.; Mao, Y.; Robinson, D. Modelling Urban Housing Stocks for Building Energy Simulation Using CityGML EnergyADE. *ISPRS Int. J. Geo-Inform.* **2019**, *8*, 163. [[CrossRef](#)]
50. AA.VV. *Informe Balance Nacional de Energía 2019*; MINEN Ministerio de Energía: Santiago, Chile, 2019. Available online: https://energia.gob.cl/sites/default/files/documentos/2020_informe_anual_bne_2019.pdf (accessed on 20 July 2023).
51. AA.VV. *Anuarios de Edificación (2010–2020)*; INE Instituto Nacional de Estadísticas: Santiago, Chile, 2020.
52. AA.VV. *Informe Final de Usos de la Energía de los Hogares en Chile*; MINEN Ministerio de Energía: Santiago, Chile, 2018.
53. Pérez-Fargallo, A.; Rubio-Bellido, C.; Pulido-Arcas, J.A.; Guevara-García, F.J. Fuel Poverty Potential Risk Index in the context of climate change in Chile. *Energy Policy* **2018**, *113*, 157–170. [[CrossRef](#)]
54. Grass, D.; Cane, M. The effects of weather and air pollution on cardiovascular and respiratory mortality in Santiago, Chile, during the winters of 1988–1996. *Int. J. Clim.* **2008**, *28*, 1113–1126. [[CrossRef](#)]
55. AA.VV. *NCh-1079: Arquitectura y Construcción—Zonificación Climática Habitacional Para Chile y Recomendaciones Para el Diseño Arquitectónico*; INN Instituto Nacional de Normalización: Santiago, Chile, 2008.
56. Villalobos, C.; Chávez, C.; Uribe, A. Energy poverty measures and the identification of the energy poor: A comparison between the utilitarian and capability-based approaches in Chile. *Energy Policy* **2021**, *152*, 112146. [[CrossRef](#)]
57. AA.VV. *Síntesis de Resultados CENSO 2017*; INE Instituto Nacional de Estadísticas: Santiago, Chile, 2018.
58. AA.VV. *Portal de Servicios Climáticos*; DMC Dirección Meteorológica de Chile: Santiago, Chile, 2022. Available online: <https://climatologia.meteochile.gob.cl/application/informacion/buscadorEstaciones> (accessed on 20 July 2023).
59. AA.VV. *Ordenanza General de Urbanismo y Construcciones OGUC*; Ministerio de Vivienda y Urbanismo MINVU, Gobierno de Chile: Santiago, Chile, 2019. Available online: <https://www.bcn.cl/leychile/navegar?idNorma=8201> (accessed on 20 July 2023).
60. AA.VV. *Plan Regulador Comunal, 2021*; Municipality of Renca: Renca, Chile, 2021. Available online: <https://renca.cl/unidades-municipales/secretaria-comunal-de-planificacion/prc/> (accessed on 20 July 2023).
61. Corporación de Desarrollo Tecnológico. *Informe Final Uso de la Energía Hogares Chile 2018*. Available online: https://energia.gob.cl/sites/default/files/documentos/informe_final_caracterizacion_residencial_2018.pdf (accessed on 20 July 2023).
62. Mutani, G.; Todeschi, V. Space heating models at urban scale for buildings in the city of Turin (Italy). *Energy Procedia* **2017**, *122*, 841–846. [[CrossRef](#)]
63. AA.VV. *Manual de Procedimientos Calificación Energética de Viviendas en Chile*, Gobierno de Chile, no. Febrero. 2018. Available online: <https://www.calificacionenergetica.cl/media/Folleto-Calificacion-Energetica-de-Viviendas.pdf> (accessed on 20 July 2023).
64. WEC World Energy Council. Available online: <https://www.worldenergy.org/transition-toolkit/world-energy-trilemma-index> (accessed on 20 July 2023).
65. Ritchie, H.; Roser, M. *Energy Production and Consumption*. 2020. Available online: <https://ourworldindata.org/energy-production-consumption> (accessed on 20 July 2023).

Disclaimer/Publisher’s Note: The statements, opinions and data contained in all publications are solely those of the individual author(s) and contributor(s) and not of MDPI and/or the editor(s). MDPI and/or the editor(s) disclaim responsibility for any injury to people or property resulting from any ideas, methods, instructions or products referred to in the content.